2018

Evaluation of binary and ternary refrigerant blends as replacements for R134a in an air-conditioning system

Ian Bell
National Institute of Standards and Technology, United States of America, ian.bell@nist.gov

Piotr Domanski
National Institute of Standards and Technology, United States of America, piotr.domanski@nist.gov

Greg Linteris
National Institute of Standards and Technology, United States of America, linteris@nist.gov

M. O. McLinden
National Institute of Standards and Technology, mark.mclinden@nist.gov

Evaluation of binary and ternary refrigerant blends as replacements for R134a in an air-conditioning system [a]

Ian BELL[1*], Piotr DOMANSKI [2], Greg LINTERIS [2], Mark McLINDEN [1]

[1] National Institute of Standards and Technology, Boulder, CO, USA
[2] National Institute of Standards and Technology, Gaithersburg, MD, USA
ian.bell@nist.gov

* Corresponding Author

ABSTRACT

We investigated refrigerant blends as possible low-GWP (global warming potential) alternatives for R134a in an air-conditioning application. We carried out an extensive screening of the binary and ternary blends possible among a list of 13 pure refrigerants comprising four hydrofluoroolefins (HFOs), eight hydrofluorocarbons (HFCs), and carbon dioxide. The screening was based on a simplified cycle model, but with the inclusion of pressure drops in the evaporator and condenser. The metrics for the evaluation were nonflammability, low-GWP, high COP (coefficient of performance), and a volumetric capacity similar to the R134a baseline system. While no mixture was ideal in all regards, we identified 14 "best" blends that were nonflammable (based on a new estimation method by Linteris, et al., presented in a companion paper at this conference) and with COP and capacity similar to the R134a baseline; the tradeoff, however, was a reduction in GWP of, at most, 51% compared to R134a. An additional eight blends that were estimated to be "marginally flammable" (ASHRAE Standard 34 classification of A2L) were identified with GWP reductions of as much as 99%. These 22 "best" blends were then simulated in a more detailed cycle model.

1. INTRODUCTION

Like all segments of society, the U.S. military is examining the options to reduce the global-warming-potential (GWP) footprint of its air-conditioning and refrigeration systems. But while much of the refrigeration industry is considering a move to refrigerants that are flammable, or at least marginally flammable, the unique operating environments of many military systems demand nonflammable replacement refrigerants. The goal of this work was to identify nonflammable, but lower-GWP, replacements for R134a in a baseline air-conditioning application while maintaining capacity and energy efficiency.

The selection of a refrigerant blend to replace refrigerant R134a is a multi-objective optimization process. There are several desired objectives:

- Minimize/eliminate flammability: As discussed in Linteris et al. (2018), the combination of the adiabatic flame temperature and the F-substitution ratio yields a prediction of the flammability class (1, 2L, 2, 3) according to the ASHRAE 34 standard (ASHRAE, 2016). It is preferred to have a flammability class designation of 1 ("no flame propagation"), but as demonstrated below, enforcing that the blend be nonflammable comes at the cost of a lower system efficiency and/or a higher GWP.
- Minimize GWP: The GWP of a blend is defined as the mass-fraction-weighted GWP of the blend's components. Several time horizons are possible for the calculation of GWP, but it is most common to consider a 100-year time horizon. The 100-year GWP values for pure fluids are tabulated in a number of sources, and here we used the values from the UN IPCC report (Myhre et al., 2013).
- Maximize COP: the coefficient of performance, or COP, characterizes the efficiency of the heat pump. The larger the COP, the better the system efficiency.

- Match the volumetric capacity Q_{vol} of the baseline system: the Q_{vol} of a heat pump is a figure of merit that is related to the size of the compressor. The larger the volumetric capacity, the smaller the compressor needs to be for a given cooling capacity.

Our search for optimal R134a replacement blends involved the above four figures of merit and consisted of the following steps:

1. Selection of pure refrigerants of low toxicity that could possibly form a replacement blend.
2. Determination of flammability classification, GWP, COP, and Q_{vol} for an exhaustive matrix of possible binary and ternary mixture compositions. In this step, we evaluated COP and Q_{vol} using a simplified cycle model.
3. Selection of "best" blends based on the blend's figures of merit.
4. Determination of COP and Q_{vol} of the "best" blends using an advanced cycle model.

2. FLUID SELECTION

Based on a comprehensive search of chemical compounds that could serve as working fluids in air-conditioning systems, McLinden et al. (2017) demonstrated that there are very limited options for low-GWP refrigerants. They identified the best working fluids based on assessments of their environmental, safety, and performance characteristics. But no single-component refrigerant was ideal in all respects; that is, no fluid was simultaneously nonflammable, low-GWP, and with good performance in an air-conditioning system. Thus, in this study, we turn to blends.

For blending, we selected 13 fluids within a range of pressure, flammability, and GWP values that might produce a blend with the desired characteristics of a R-134a replacement. These included hydrofluoroolefins (HFOs), which have very low GWP values (≈1 relative to CO_2), but that are mildly flammable; hydrofluorocarbons (HFCs) with moderate-to-high GWP values that were nonflammable and thus, might serve to suppress the flammability of a blend; additional mildly flammable HFCs; and carbon dioxide (CO_2), which is nonflammable with GWP = 1, but which would raise the working pressure of a blend. All the selected fluids were of low toxicity (*i.e.*, an "A" classification under ASHRAE Standard 34 (ASHRAE, 2016)). Additional considerations were the commercial availability of the fluid and the availability of property data (in the form of an accurate equation of state), so that cycle simulations could be carried out with some measure of confidence.

The list of candidate working fluids considered in this study is summarized in Table 1. The global warming potential values (based on a 100-year horizon) were taken from the IPCC report on climate change (Myhre et al., 2013).

Table 1: Pure fluids selected in this study and some of their characteristics (T_c: critical temperature)

ASHRAE designation	long name	formula	T_c/K	GWP_{100}	ASHRAE classification
R134a	1,1,1,2-tetrafluoroethane	CF_3CH_2F	374.2	1300	A1
R227ea	1,1,1,2,3,3,3-heptafluoropropane	CF_3CHFCF_3	374.9	3350	A1
R125	pentafluoroethane	CHF_2CF_3	339.2	3170	A1
R143a	1,1,1-trifluoroethane	CF_3CH_3	345.9	4800	A2L
R32	difluoromethane	CH_2F_2	351.3	677	A2L
R152a	1,1-difluoroethane	CHF_2CH_3	386.4	138	A2
R134	1,1,2,2-tetrafluoroethane	CHF_2CHF_2	391.8	1120	Not assigned
R41	fluoromethane	CH_3F	317.3	116	Not assigned
R1234yf	2,3,3,3-tetrafluoropropene	$CF_3CF=CH_2$	367.9	1	A2L
R1234ze(E)	trans-1,3,3,3-tetrafluoropropene	$CHF=CHCF_3$ (trans)	382.5	1	A2L
R1234ze(Z)	cis-1,3,3,3-tetrafluoropropene	$CHF=CHCF_3$ (cis)	423.3	1	Not assigned
R1243zf	3,3,3-trifluoropropene	$CF_3CH=CH_2$	376.9	1	Not assigned
R744	carbon dioxide	CO_2	304.1	1	A1

3. ESTIMATED FIGURES OF MERIT OF THE BLENDS

3.1 Simplified Cycle Model

The cycle model is based upon a simplified analysis of a four-component heat pump system with lumped pressure drops. A schematic of the system is shown in Fig. 1, and $\log(p)$-h and T-s property figures are shown in Fig. 2. Due to the subtle complexities of modeling blends in thermodynamic cycles, we describe the cycle model in detail below. The specification of the model parameters is as follows:

- Evaporator dew-point temperature $T_{\text{evap,dew}}$: 10 °C
- Condenser bubble-point temperature $T_{\text{cond,bub}}$: 40 °C
- Evaporator outlet superheat ΔT_{sh}: 5 K
- Condenser exit subcooling ΔT_{sc}: 7 K
- Compressor adiabatic efficiency η_{a}: 0.7
- Evaporator pressure drop: for the baseline system, a reduction in dew-point temperature of 2 K
- Condenser pressure drop: for the baseline system, a reduction in bubble-point temperature of 2 K

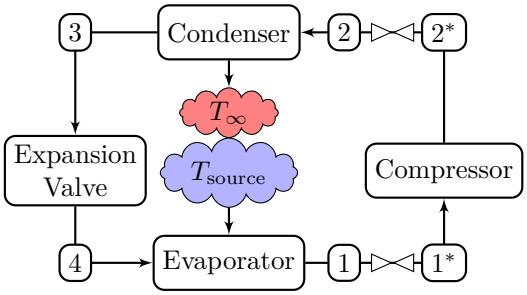

Figure 1: System schematic. The state point indices 1, 2, etc. correspond to the labeled state points in Fig. 2.

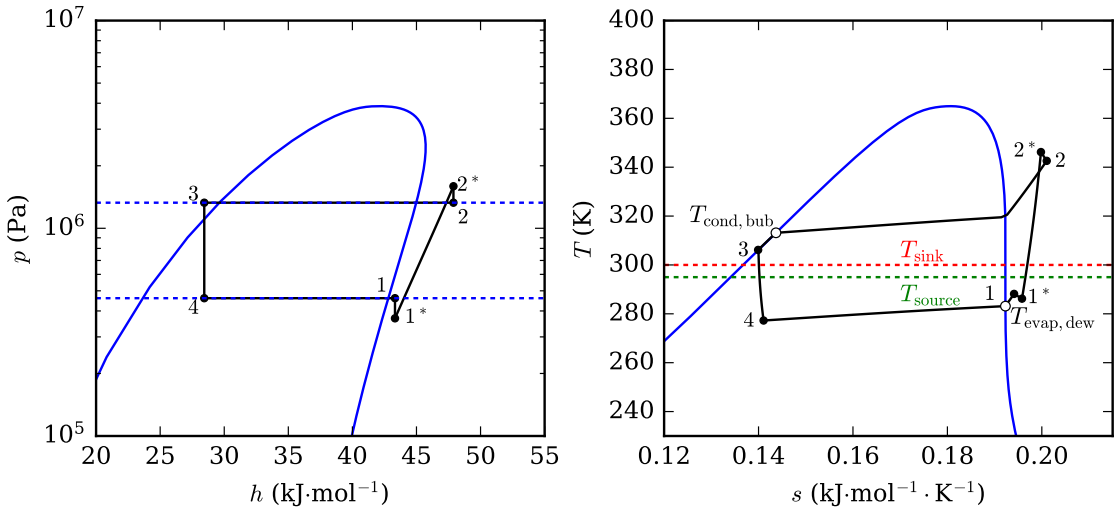

Figure 2: p-h and T-s cycle diagrams for an equimolar mixture of R125 + R1234ze(E). Calculations are carried out with NIST REFPROP (Lemmon et al., 2018).

The key difference between this cycle model and other simplified cycle models is the inclusion of a simplified pressure drop model. It is assumed that the pressure drop from the high-side components and the low-side components can be lumped into pressure drops at the outlet and inlet of the compressor, respectively. Therefore the compressor sees a larger pressure lift than the pressure ratio corresponding to the pressures in the evaporator and condenser. The drop in saturation temperature for high- and low-sides of the system are specified for the baseline R134a system, and the pressure drop scaling (described below) is used to calculate the pressure drop for the refrigerant blends.

In the simplified cycle analysis, the pressures in the evaporator and the condenser are assumed to be constant, given by vapor-liquid equilibrium calculations at the respective saturation pressure

$$p_{\text{evap}} = p_{\text{dew}}(T_{\text{evap,dew}}) \tag{1}$$

$$p_{\text{cond}} = p_{\text{bub}}(T_{\text{cond,bub}}). \tag{2}$$

The selection of the saturation states used to define the low- and high-side pressures is based on a rudimentary pinch analysis. This pinch analysis assumes that the source and sink temperatures are fixed, that the condenser outlet pinch is fixed, and that the evaporator outlet pinch is fixed. Therefore, stacking up the temperature differences (plus the respective superheating or subcooling), we can arrive at the relevant saturation temperature. This method is the worst-case simplified cycle analysis option for mixtures with temperature glide (McLinden and Radermacher, 1987) because the heat-transfer irreversibilities are maximized. This represents a conservative approach in the sense that it favors drop-in replacements that would require little or no modifications of existing systems. For blends having significant temperature glide, and systems with counterflow or cross-counterflow heat exchange, the temperature profiles of the source and sink fluids and that of the working mixture may be better aligned, resulting in lower heat transfer irreversibilities and higher efficiencies.

Condenser The outlet enthalpy of the condenser is given by

$$h_3 = h(T_3, p_{\text{cond}}), \tag{3}$$

where the outlet temperature of the condenser T_3 is given by

$$T_3 = T_{\text{cond,bub}} - \Delta T_{\text{sc}}, \tag{4}$$

and where the bubble-point temperature of the condenser is given by

$$T_{\text{cond,bub}} = T_{\text{bub}}(p_{\text{cond}}). \tag{5}$$

The pressure drop in the condenser (Δp_{high}) is given by Eq. (15), in which ρ'' and μ'' are evaluated at the dew point at the condensing pressure p_{cond}.

Evaporator The dew-point temperature is imposed for the evaporator, as is its inlet enthalpy (because the outlet state of the condenser is fully specified and the throttling process is assumed to be adiabatic). Therefore the states 3, 4, and 1 can be fully specified and the enthalpies calculated from

$$h_4 = h_3 \tag{6}$$

$$h_1 = h(T_{\text{evap}} + \Delta T_{\text{sh}}, p_{\text{evap}}) \tag{7}$$

The pressure drop in the evaporator Δp_{low} is given by the relationship in Eq. (15), in which ρ'' and μ'' are evaluated at the dew point at the evaporation pressure p_{evap}.

Compressor The pressure drops in the cycle are lumped at the compressor. Therefore, the inlet state of the compressor 1^* is given by the pressure drop relative to the state point 1:

$$h_{1^*} = h_1 \tag{8}$$

$$T_{1^*} = T(h_{1^*}, p_{\text{evap}} - \Delta p_{\text{low}}) \tag{9}$$

Similarly, the outlet pressure of the compressor p_{2^*} is given by $p_{2^*} = p_{\text{cond}} + \Delta p_{\text{high}}$. The classical adiabatic efficiency formulation is used for the compressor, assuming that there is no heat transfer from the compressor to the environment. Therefore, the adiabatic efficiency is defined by

$$\eta_a = \frac{h_{2\text{s}} - h_{1^*}}{h_{2^*} - h_{1^*}}, \tag{10}$$

where the isentropic enthalpy $h_{2\text{s}}$ is obtained from

$$h_{2\text{s}} = h(s_{1^*}, p_{2^*}). \tag{11}$$

Cycle metrics The COP of the air conditioner is given by

$$\text{COP} = \frac{h_1 - h_4}{h_{2^*} - h_{1^*}} \tag{12}$$

and the volumetric capacity of the heat pump is given by

$$Q_{\text{vol}} = (h_4 - h_1) \cdot \rho(T_{1^*}, p_{1^*}) \tag{13}$$

Pressure drop modeling As demonstrated by McLinden et al. (2017), the inclusion of pressure drop in the model (even if highly approximate), is crucial to yield a fair screening of refrigerants. The simplified pressure drop in our analysis is based upon scaling the system for the refrigerant blends to have the same capacity as the baseline R134a system.

The pressure drop in each of the heat exchangers is assumed to be based upon a frictional pipe flow analysis of a homogeneous fluid (making use of the Fanning friction factor f_F, and neglecting accelerational pressure drop) given by

$$\Delta p = \frac{2 f_F G^2 L}{\rho D} = \frac{2L}{D} \frac{\dot{m}^2}{A^2} \frac{1}{\rho} f_F. \tag{14}$$

For a specified pressure drop Δp and equality of system cooling capacity $Q = \dot{m}/(h_1 - h_4)$, after canceling all non-thermophysical properties and lumping them into a constant, the system specific term $C_{\Delta p}$ is given by

$$C_{\Delta p} = \frac{\Delta p \rho'' (h_1 - h_4)^{1.8}}{\mu''^{0.2}}, \tag{15}$$

which is obtained for the baseline system (all units are base SI), for an imposed pressure drop given as a change in saturation temperature for R134a. The pressure drop coefficient obtained is then used for all of the blends, where the thermophysical properties (density ρ'' and viscosity μ'') are evaluated at the dew point state at the specified heat exchange pressure.

3.2 Estimation of Flammability

The refrigerant flammability prediction of Linteris et al. (2018) uses two parameters that can be readily evaluated: the adiabatic flame temperature T_{ad} and the ratio of the number of fluorine atoms to the total of fluorine plus hydrogen atoms in the refrigerant blend, F/(F + H). T_{ad} is calculated from the enthalpy of the reactants and products, via `cantera` (Goodwin et al., 2017), an open-source software package for problems involving chemical kinetics, thermodynamics, and transport properties. The calculation of the F/(F + H) ratio is a simple mathematical evaluation calculated from the chemical formulas of the blend components and their mole fractions. A plot of T_{ad} vs F/(F+H) is constructed, with each point representing a refrigerant, as shown in Fig. 3. Less flammable compounds are in the lower right of the plot, and more flammable, the upper left. The flammability of the refrigerant is represented by the slope of the line between an origin (at (F/(F + H)) = 0 and T_{ad} = 1600 K and the point in question. The origin point is based on the observation that hydrocarbons (for which (F/(F + H)) = 0) do not burn when diluted with an inert gas such that their adiabatic flame temperature falls below 1600 K. For more details, please see Linteris et al. (2018).

Figure 3 shows the three ASHRAE Standard 34 flammability classes 1, 2L, and 2/3. Assessment of pure fluids and blends having an ASHRAE 34 classification are presented, based on their T_{ad} and F/(F + H), with mixtures evaluated at their nominal blend compositions. As indicated, the present flammability estimation appears to represent the ASHRAE 34 data reasonably well.

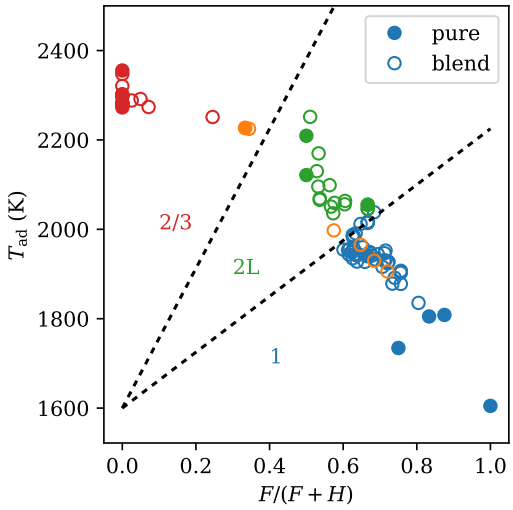

Figure 3: Estimation of blend flammability based on adiabatic flame temperature T_{ad} versus F/(F+H) for pure fluids and nominal blend compositions specified in the ASHRAE 34 standard (ASHRAE, 2016). The colors correspond to the flammability class – 1: blue, 2L: green, 2: orange, 3: red.

3.3 Screening Results

The screening involved an extensive evaluation, using the simplified cycle model described in Section 3.1, of all possible combinations of the 13 fluids listed in Table 1 taken two or three at a time (*i.e.*, all possible binary and ternary mixtures). A composition interval of 0.04 mole fraction was applied to yield a total of 100,387 mixtures to be evaluated. The simplified cycle calculations were carried out in parallel in Python with the `multiprocessing` Python package[b]. The flammability analysis of Linteris et al. (2018) was then applied to estimate the flammability class of the blend.

The screening resulted in a large dataset of binary and ternary mixtures, and for each mixture, an assessment of their figures of merit (flammability class, GWP, COP, and Q_{vol}). The production of this set of data was, in some sense, the easy part of this study; much more difficult was the determination of the "best" refrigerant blend(s). In truth, the selection of the "best" blend depends largely on how the user weights the available figures of merit.

Figure 4 provides an overview of the results for the mixtures formed of the 13 components in Table 1. This figure presents a scatter plot of the COP versus Q_{vol} results for the studied blends sorted into nine "bins" of GWP and flammability. Additional blends had GWP > 1300 and are not shown in Fig. 4. In the upper left hand corner of the figure are mixtures that are probably nonflammable according to the flammability assessment of Linteris et al. (2018) and have a GWP < 150, *i.e.*, less than 12% that of refrigerant R134a.

Figure 5 shows a graphical representation of the prevalence of each component in the different bins. The larger the radius of a wedge, the more prevalent the component is in the mixtures in that bin. In many of the bins there are certain components that dominate the bin. For instance, the low-GWP, nonflammable bin is dominated by carbon dioxide (R744), and the low-GWP, moderately flammable bin is dominated by the HFOs. Each time a component occurs in a bin, its mole fraction in the mixture is added to the running sum for that bin. The mole-fraction-weighted prevalences are then normalized within the bin in order to yield the relative prevalence of each component.

[b]\https://docs.python.org/3/library/multiprocessing.html

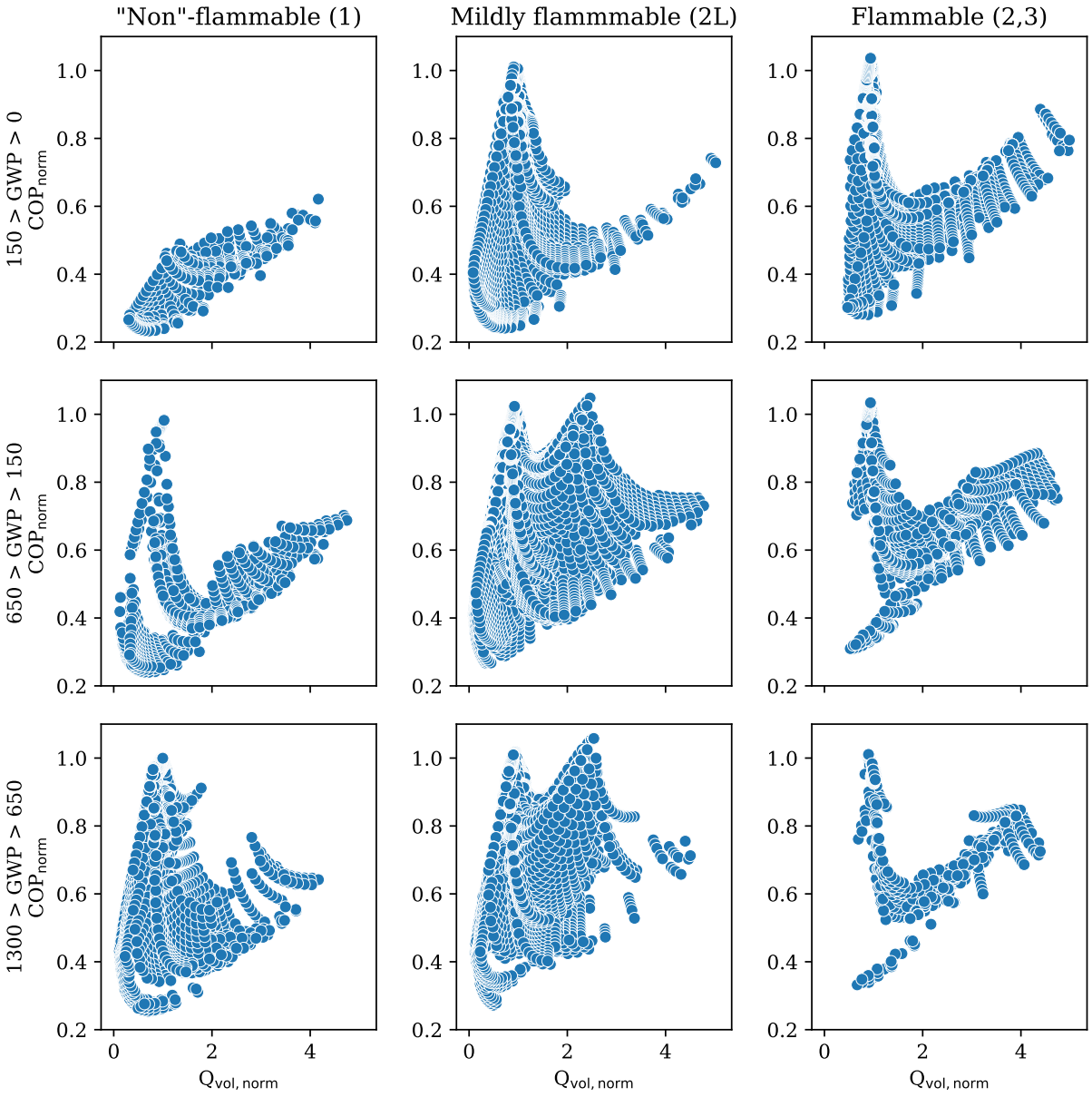

Figure 4: An overview of the cycle figures of merit for the binary and ternary blends studied, divided into bins of GWP and estimated flammability. The "best" bin is at the upper left, and the bins moving towards the lower right are worse according to our objective functions. Values of the volumetric capacity and COP are normalized by the value for the baseline R134a system.

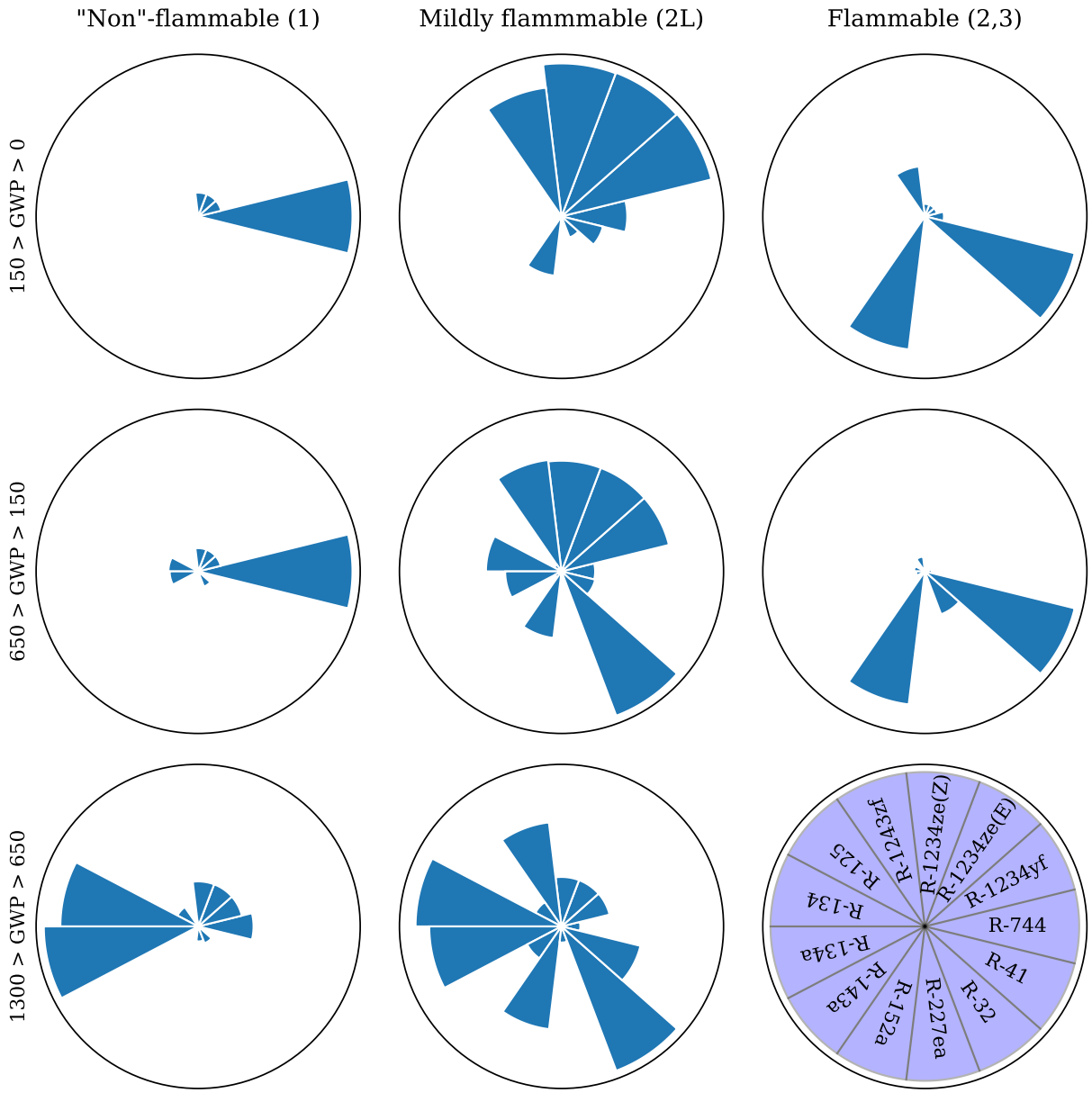

Figure 5: Radial histograms showing the prevalence of each component in each of the bins. The key in the lower right corner is aligned with the radial histograms in each bin.

3.4 Selection of "Best" Blends

We were not able to identify any blends that met all of our desired constraints. The mixtures in the non-flammable/low GWP bin (upper-left corner of Fig. 4) meet two of the desired objectives, but they suffer from a much lower efficiency than the baseline R134a system and were dropped from further consideration. Thus, to define the "best" blends we selected the nonflammable blends having the highest COP within a range of GWP values from 643 to 870 (*i.e.*, from the remaining two bins in the left column of Fig. 4). These 14 "best blends" are listed in Table 2. Note that we did not separately select blends having very similar compositions to the "best" blends unless they offered a distinct advantage in one or more of our metrics.

If one is willing to tolerate a probable 2L flammability classification according to the ASHRAE 34 standard, there are low GWP options that yield efficiency near that of the baseline R134a system (*i.e.*, the top two rows of the middle column in Fig. 4). We also selected eight additional blends that were marginally flammable with GWP values ranging from 8 to 573. All this is to say that the search for the "perfect" refrigerant blend continues.

4. DETAILED CYCLE SIMULATIONS

4.1 Model Description

We performed detailed cycle simulations using the CYCLE_D-HX model (Brown et al., 2017) on the "best" blends described in Section 3.4. In contrast to the simplified vapor compression cycle model, which requires refrigerant saturation temperatures in the evaporator and condenser as inputs, CYCLE_D-HX establishes saturation temperatures in the heat exchangers using the specified temperatures profiles of the heat source and heat sink (*i.e.*, the conditioned and outdoor air) and the mean effective temperature differences (ΔT_{hx}) in the evaporator and condenser. This representation of heat exchangers facilitates the inclusion of both thermodynamic and transport properties in cycle simulations (Brown et al., 2002a,b; Brignoli et al., 2017). The evaporator and condenser can be counterflow, crossflow, or parallel flow, although only cross-flow is simulated here. During the iteration procedure, CYCLE_D-HX calculates ΔT_{hx} for each heat exchanger from (Domanski and McLinden, 1992):

$$\frac{1}{\Delta T_{hx}} = \frac{Q_1}{Q_{hx}\Delta T_1} + \frac{Q_2}{Q_{hx}\Delta T_2} + \cdots = \frac{1}{Q_{hx}} \sum_i \frac{Q_i}{\Delta T_i} \tag{16}$$

In this equation, ΔT_{hx} is a harmonic mean weighted with the fraction of heat transferred in individual sections of the heat exchanger, based on the assumption of a constant overall heat-transfer coefficient throughout the heat exchanger. Each term represents the contribution of a heat exchanger section. At the outset, the model calculates ΔT_{hx} based on sections corresponding to the subcooled liquid, two-phase, and superheated regions. Then, the model bisects each section and uses Eq. (16) to calculate a new value of ΔT_{hx}. The model repeatedly bisects each subsection until the ΔT_{hx} obtained from two consecutive evaluations agree within a convergence parameter. As an alternative to specifying ΔT_{hx}, the heat exchangers can be characterized by the overall heat conductance $UA_{hx} = 1/R_{hx}$ (R_{hx} being the total resistance to heat transfer in the heat exchanger). In this case, the model calculates the corresponding ΔT_{hx} from the basic heat-transfer relation, $\Delta T_{hx} = Q_{hx}/UA_{hx}$, where Q_{hx} is the product of refrigerant mass flow rate and enthalpy change in the evaporator or condenser, as appropriate. The representation of heat exchangers by their UA_{hx} allows for inclusion of refrigerant heat transfer and pressure drop characteristics in comparable evaluations of different refrigerants. For this purpose, CYCLE_D-HX considers R_{hx} as the summation of the resistance on the refrigerant side (R_r), and combined resistances of the heat exchanger material and heat-transfer-fluid (HTF) side, ($R_{tube} + R_{HTF}$)

$$R_{hx} = R_r + (R_{tube} + R_{HTF}) \tag{17}$$

$$R_r = 1/(\alpha_r \cdot A_r) \tag{18}$$

where α_r is the refrigerant heat-transfer coefficient in $W \cdot m^2 \cdot K^{-1}$ and A_r is the surface area on the refrigerant side in m^2.

The refrigerant heat-transfer resistance R_r varies with operating conditions and the refrigerant, but the other resistances ($R_{tube} + R_{HTF}$) are assumed to be constant. Their combined value can be calculated from UA_{hx}, α_r, and A_r values during a simulation run for the "reference" refrigerant, for which the heat exchanger's ΔT_{hx} are known from laboratory measurements and were provided as input. CYCLE_D-HX calculates ($R_{tube} + R_{HTF}$) for the evaporator and condenser within

Table 2: Detailed results from CYCLE_D-HX

Blend components	Composition (molar)	GWP_{100}	COP/COP_{R134a}	$Q_{vol}/Q_{vol,R134a}$
Class 1 nonflammable (predicted)				
R134a/1234yf/134	0.48/0.48/0.04	634	0.987	0.975
R134a/1234yf/1234ze(E)	0.52/0.32/0.16	640	0.987	0.989
R134a/1234yf	0.52/0.48	640	0.989	1.029
R134a/1234yf/134	0.40/0.44/0.16	665	0.986	0.958
R134a/125/1234yf	0.44/0.04/0.52	676	0.985	1.049
R134a/227ea/1234yf	0.40/0.04/0.56	681	0.984	1.007
R134a/1234ze(E)	0.60/0.40	745	0.988	0.908
R134a/1234yf	0.60/0.40	745	0.990	1.031
R134a/1234ze(E)/1243zf	0.60/0.36/0.04	750	0.990	0.966
R134a/R1234yf/1234ze(E)	0.64/0.2/0.16	799	0.990	0.986
R134a/152a/1234yf	0.64/0.04/0.32	817	0.993	1.023
R134a/1234yf/134	0.52/0.32/0.16	825	0.990	0.966
R134a/1234ze(E)	0.68/0.32	852	0.991	0.929
R134a/1234yf/1243zf	0.68/0.2/0.12	870	0.994	1.020
Class 2L flammable (predicted)				
R152a/1234yf	0.08/0.92	8	0.980	0.957
R134a/1234yf	0.20/0.80	238	0.980	0.996
R134a/152a/1234yf	0.20/0.16/0.64	270	0.987	0.984
R152a/1234yf/134	0.16/0.48/0.36	418	0.984	0.900
R134a/1234yf	0.36/0.64	436	0.985	1.018
R134a/1234yf/1243zf	0.36/0.44/0.20	451	0.988	1.004
R134a/152a/1234yf	0.36/0.20/0.44	496	0.994	0.994
R134a/1234yf	0.468/0.532	573	0.988	1.027

this "reference run" and stores their values for use in subsequent simulation runs for calculation of UA_{hx} characterizing the heat exchangers with a new refrigerant or operating conditions.

CYCLE_D-HX requires the following operational input data for the "reference run": HTF inlet and outlet temperatures for the evaporator and condenser; ΔT_{hx} for the evaporator and condenser (to achieve the measured evaporator and condenser saturation temperatures); evaporator superheat and pressure drop; and condenser subcooling and pressure drop. Additional "reference run" inputs include compressor isentropic and volumetric efficiencies, and electric motor efficiency. Heat exchanger geometry inputs include the tube inner diameter and length, the number of refrigerant circuits, and the total length of heat exchanger tubing.

CYCLE_D-HX also optimizes the coil circuiting in the evaporator and condenser to maximize the system's COP. This option represents a design environment where the HTF and number of refrigerant tubes remains constant, but the tube connections and refrigerant mass flux can be changed. Using this option, the model provides information on the relative performance potentials of refrigerants operating in systems with serpentine air-to-refrigerant heat exchangers.

4.2 Simulation Results

The series of CYCLE_D-HX simulations of the 22 "best" blends started with R134a simulations, which served as the "reference" refrigerant. For this purpose, we established an R134a system, with operating parameters approximating those used in the simplified cycle simulations: the same evaporator outlet superheat (5 K), condenser exit subcooling (7 K) and compressor efficiency (0.7) were used; however, refrigerant pressure drop (corresponding to 2 K drop in saturation temperature) was imposed in the heat exchangers (as opposed to the compressor suction and discharge sides), and average two-phase temperatures in the heat exchangers were considered as opposed to the dew-point temperature (evaporator) and bubble-point temperature (condenser). The circuitry in the R134a system was optimized to attain the maximum COP, and the performance of this R134a optimized system became the reference for normalization of COP and Q_{vol} of the nineteen blends.

Table 2 presents GWP and simulation results for the nineteen blends. For the nonflammable group, the normalized values for COP and Q_{vol} were in the 0.984 – 0.994 and 0.908 – 1.049 range, respectively, with the GWP values ranging from 634 to 870. The main component of all of these blends is R134a. The other components are the HFOs R1234yf, R1234ze(E), and R1243zf and HFCs R152a and R134; R125 and R227ea appear at a low concentration in one blend each. For the mildly flammable group, the GWP values range from 8 to 573, and the normalized COP ranges from 0.980 to 0.994. The normalized $Q_{vol}$the blends in this group are in the range 0.900 – 1.027. These blends comprise R134a as the main component along with R1234yf, and R152a; R134 and R1243zf appear in one blend each.

Keeping in mind that the main goal of this study was to find a nonflammable, low-GWP replacement with a comparable COP and Q_{vol} of that for R134a in an air-conditioning application, the lowest GWP among the suitable nonflammable blends is 634, a 51% reduction in GWP compared with R134a. The blend R134a/1234yf, with molar composition (0.468/0.532) and GWP = 573, was predicted to be marginally flammable by our estimation method; this blend is designated R513A by ASHRAE Standard 34 with a classifcation of A1 (i.e., nonflammable).

If one is willing to tolerate a probable 2L flammability classification according to the ASHRAE 34 standard, there are options that yield efficiency near that of the baseline R134a system with GWP of 8 and 4.3 % lower Q_{vol}. Similarly, if a more moderate reduction in GWP is acceptable, there are higher-pressure low-GWP options with R32 that attain a similar COP as R134a with a more than doubled Q_{vol} (i.e., the fluids making up the second COP maxima shown in the middle panel of Figure 4.)

5. CONCLUSIONS

Our search for nonflammable low-GWP replacements for R134a in an air-conditioning system yielded several blends with COP and Q_{vol} similar to those of R134a. The GWP of the identified nonflammable blends were in the 634 - 870 range. Among the mildly flammable (2L) blends, GWP reductions of up to a factor of 100 relative to R134a were identified.

The study was limited to binary and ternary blends formed from a set of 13 pure fluids currently available in NIST REFPROP (Lemmon et al., 2018). Additional pure fluids, such as those identified by McLinden et al. (2017), should be considered once sufficient experimental data become available to build the thermodynamic equations of state and mixture models required to implement them into REFPROP.

The COP and Q_{vol} values calculated from CYCLE_D-HX model present the relative performance potential of the considered fluids in a system with air-to-refrigerant heat exchangers. Experimental validation of these findings and predicted flammability classifications is merited.

Finally, flammability limits are generally device-dependent, so while the current estimation method can predict the behavior of a mixture in the ASTM E681 test protocol (for constituents which are chemically similar to those used to develop the model; i.e., hydrocarbons, HFCs, HFOs, etc.), the behavior of the mixtures in other flammability tests or actual full-scale configurations having more powerful ignition sources, clutter, turbulence, etc., may not be predicted as well. Moreover, since there is uncertainty in the flammability behavior and prediction for compounds near the flammability boundary, the actual ASHRAE Standard 34 flammability behavior predicted in the present work should ultimately be verified experimentally.

ACKNOWLEDGMENTS

This work was supported by the U.S. Department of Defense, Strategic Environmental Research and Development Program (SERDP), project WP-2740.

REFERENCES

ASHRAE (2016). ANSI/ASHRAE Standard 34-2016 Designation and Safety Classification of Refrigerants.

Brignoli, R., Brown, J. S., Skye, H. M., and Domanski, P. A. (2017). Refrigerant performance evaluation including effects of transport properties and optimized heat exchangers. Int. J. Refrig, 80:52–65.

Brown, J., Kim, Y., and Domanski, P. (2002a). Evaluation of Carbon Dioxide as R22 Substitute for Residential Conditioning. ASHRAE Transactions, 108(2):954–963.

Brown, J. S., Brignoli, R., and Domanski, P. A. (2017). CYCLE_D-HX: NIST vapor compression cycle model accounting for refrigerant thermodynamic and transport properties, version 1.0, user's guide. Technical Report 1974, NIST.

Brown, J. S., Yana-Motta, S. F., and Domanski, P. A. (2002b). Comparitive analysis of an automotive air conditioning systems operating with CO_2 and R134a. Int. J. Refrig., 25(1):19–32.

Domanski, P. A. and McLinden, M. O. (1992). A simplified cycle simulation model for the performance rating of refrigerants and refrigerant mixtures. Int. J. Refrig, 15(2):81–88.

Goodwin, D. G., Moffat, H. K., and Speth, R. L. (2017). Cantera: An Object-oriented Software Toolkit for Chemical Kinetics, Thermodynamics, and Transport Processes. http://www.cantera.org. Version 2.3.0.

Lemmon, E. W., Bell, I. H., Huber, M. L., and McLinden, M. O. (2018). NIST Standard Reference Database 23: Reference Fluid Thermodynamic and Transport Properties-REFPROP, Version 10.0, National Institute of Standards and Technology.

Linteris, G., Bell, I., McLinden, M., and Domanski, P. (2018). An Empirical Model For Refrigerant Flammability Based On Molecular Structure and Thermodynamics. In 17th International Refrigeration and Air Conditioning Conference at Purdue, July 9-12, 2018.

McLinden, M. and Radermacher, R. (1987). Methods for comparing the performance of pure and mixed refrigerants in the vapour compression cycle. International Journal of Refrigeration, 10(6):318 – 325.

McLinden, M. O., Brown, J. S., Brignoli, R., Kazakov, A. F., and Domanski, P. A. (2017). Limited options for low-global-warming-potential refrigerants. Nat. Commun., 8:14476.

Myhre, G., Shindell, D., Bréon, F.-M., Collins, W., Fuglestvedt, J., Huang, J., Koch, D., Lamarque, J.-F., Lee, D., Mendoza, B., Nakajima, T., Robock, A., Stephens, G., Takemura, T., and Zhang, H. (2013). Anthropogenic and Natural Radiative Forcing. Cambridge University Press, Cambridge, United Kingdom and New York, NY, USA.

NOMENCLATURE

Variables

A	cross-sectional area (m^2)
A_r	surface area on the refrigerant side (m^2)
$C_{\Delta p}$	pressure drop constant
COP	coefficient of performance (-)
D	diameter (m)
G	mass flux ($kg^2 \cdot s^{-1} \cdot m^{-2}$)
f_F	Fanning friction factor (-)
GWP	global warming potential (-)
h	mass specific enthalpy ($J \cdot kg^{-1}$)
L	length (m)
$\dot{m}$	mass flow rate ($kg \cdot s^{-1}$)
p	pressure (Pa)
Δp	pressure difference (Pa)
Q	capacity (W)
Q_{vol}	volumetric capacity ($W \cdot m^{-3}$)
R	heat-transfer resistance ($K \cdot W^{-1}$)
s	mass specific entropy ($J \cdot kg^{-1} \cdot K^{-1}$)
ΔT	temperature difference (K)
T	temperature (K)
UA	overall heat conductance ($W \cdot K^{-1}$)
α_r	refrigerant heat-transfer coefficient ($W \cdot m^2 \cdot K^{-2}$)
μ''	viscosity of saturated vapor (Pa·s)
ρ	mass density ($kg \cdot m^{-3}$)
ρ''	mass density of saturated vapor ($kg \cdot m^{-3}$)
η_a	adiabatic efficiency (-)

Subscripts

ad	adiabatic flame temperature
bub	bubble
c	critical
cond	condenser
evap	evaporator
hx	heat exchanger
r	refrigerant
vol	volumetric
sc	subcooling
sh	superheat
1-4	state points
2s	isentropic compression
1*, 2*	state points with pressure drop